Form Closure For Fully Actuated and Robust Obstacle-Aided Locomotion in Snake Robots

Jostein Løwer[1], Irja Gravdahl[1], Damiano Varagnolo[1] and Øyvind Stavdahl[1]

Abstract—In this paper we adapt the theory of form closure to define the form closed region: The subset of a snake robot's configuration space for which the constraints imposed by the obstacles in its environment render the system fully actuated. We show that the identification of form closed configurations is numerically feasible, and introduce the relaxed condition of form boundedness to achieve robustness in the presence of model uncertainties. We moreover show an example application where the concept of form closed region is used to produce predictable constrained motion in a cluttered environment using lateral undulation.

Index Terms—Biologically-Inspired Robots, Biomimetics, Multi-Contact Whole-Body Motion Planning and Control

I. INTRODUCTION

SNAKE robots aspire to inherit the unique abilities of their biological counterparts. These abilities may include maneuvering in rugged and complex terrain that is inaccessible for legged or wheeled robots, move in narrow and enclosed spaces and possibly climb complex structures [1]. Currently this is a largely unrealized potential. Like biological snakes, these robots move using an array of different propulsion techniques [2]. This paper specifically focuses on one genre of snake robot locomotion called *Obstacle-Aided Locomotion* (OAL) [3]. The overarching goal of OAL is for the snake robot to propel itself by pushing its body against obstacles in a cluttered environment as shown in Figure 1.

Control strategies for snake robots are typically complex, as the joints of the robots may be actuated directly, but the position and orientation of the snake in its ambient space generally constitute unactuated degrees of freedom. A snake robot may also have complex interaction with the obstacles in its environment, which further complicates the system's kinematics by introducing discontinuous contact constraints. The overall goal of this paper is to identify computationally feasible regions of the robots' configuration space in which the kinematics of the robot can be simplified, in order to make OAL control strategies more tractable.

To this end we utilize the concept of form closure [4] to identify the *form closed region*: a subset of a robots' configuration space that renders the system fully actuated by leveraging the constraints imposed by obstacles in its environment. A robot that is limited in motion to the form
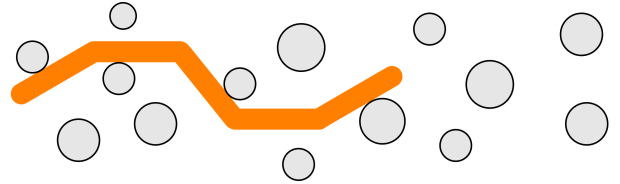
Fig. 1. An articulated snake robot (orange) seen from above, in a planar environment cluttered by obstacles. This article deals with the question of how the robot joints may be actuated to produce robust locomotion leveraging the obstacles in such environments.

closed region exhibits several properties that are beneficial in motion planning and OAL, which are covered in this paper. Subsequently, we identify the *form bounded region* that has similar properties as the form closed region under more relaxed conditions.

Form closure has found diligent use in the field of prehensile robotic gripping, and is widely used as a method for calculating suitable grasps for manipulating objects with different geometries [5], [6]. This paper covers only the case of planar snake robots, but we show that the findings in this paper can be generalized to a three-dimensional workspace.

The structure of the paper is as follows: Section II gives a brief review of the state-of-the art in snake robot modeling and locomotion. Sections III and IV derive a model of a planar snake robot with environmental constraints, adapt the theory of from closure to planar snake robots, and introduce the concept of form boundedness. The numerical calculation of form closure is addressed in Section V. In Section VI we show an application of form closure in a planar case, exploiting form closure to guarantee constrained locomotion in cluttered environment using lateral undulation. Section VII discusses the findings of this paper, identifies potential limitations and outlines future work. The main contributions of this paper are covered in Section III through Section VII.

II. RELATED WORKS

The history and application of different locomotion strategies have been thoroughly documented in a recent review on snake robots [1]. Because of this, we limit this section to works that have been published since the review, and ones directly pertaining to OAL or similar concepts.

The term OAL was first introduced in [3] and further explored in the subsequent works [7]–[9]. The hybrid dynamics of a snake robot in contact with obstacles was first visited in [8], and the modeling of snake robots for Hybrid Position-Force Control was studied in [10]. In [11], a piecewise helical motion is used to produce OAL in a cluttered

planar environment. More recently, the findings in [12] show a strategy for locomotion applying theory from geometric mechanics in a scenario similar to the one studied in this paper. The work in [13] relates closely to the fundamental ideas of OAL, where traveling waves are used to propel a snake robot through virtual "hoops". A method for perception-driven path planning for OAL was proposed in [14].

Recent works pertaining to snake locomotion, but only indirectly to OAL, include a study that shows how concertina-like locomotion can be used for mobile manipulation [15], a study on path following using anisotropic friction on planar surfaces [16] and a study on helical rolling in straight pipes [17]. A similar approach for locomotion in pipes using trapezoidal-like waves can be found in [18]. Adaptive control for under-actuated snake robots has been explored in [19]. We also note the works [20], [21] that study the interaction of snake robots with obstacles, but are not included in the review of [1].

Form closure was used to calculate grasps when using the body of a snake robot as a gripping mechanism in [22]. However, to the best of our knowledge, the present study is the first to demonstrate the use of form closure and related concepts for locomotion purposes.

The term "Form-closed region" was previously used in the field of mechanical forming processes [23], however, it bears little resemblance to the concept of the form closed region as defined in this paper except in name.

III. MODELING OF SNAKE ROBOTS UNDER ENVIRONMENTAL CONSTRAINTS

Consider a planar snake robot that inhabits a planar workspace $\mathcal{W} = \mathbb{R}^2$. We study this system in a compact timeframe $\mathcal{T} \subset \mathbb{R}$ with t representing a point of time in $\mathcal{T}$. The robot is comprised of N links connected by $N-1$ joints, indexed from tail to head, as shown in Fig. 2. We model these as an open kinematic chain of N links where the joints are placed where two consecutive links meet. The joint angles are given by

$$\boldsymbol{\phi} = (\phi_1 \dots \phi_{N-1}) \in \mathcal{Q}_\phi$$

where ϕ_i is the relative angle between the two links interconnected by joint i and $\mathcal{Q}_\phi = \mathbb{R}^{N-1}$. The robot's *pose* in relation to its environment can be defined by the vector

$$\boldsymbol{q}_N = (\boldsymbol{x}_N, \boldsymbol{y}_N, \boldsymbol{\theta}_N) \in \mathcal{Q}_N \quad (1)$$

where $(\boldsymbol{x}_N, \boldsymbol{y}_N) \in \mathcal{W}$ is the position of the robot's head in the workspace and θ_N is the orientation of the its head relative to the world frame. As the angle θ_N is a cyclic coordinate, $\mathcal{Q}_N$ is diffeomorphic to the Special Euclidean Group SE(2). The complete configuration of the robot is given by the generalized coordinate $\boldsymbol{q}$ that is defined as

$$\boldsymbol{q} = (\boldsymbol{\phi}, \boldsymbol{q}_N) \in \mathcal{Q} \quad (2)$$

where $\mathcal{Q} = \mathcal{Q}_\phi \times \mathcal{Q}_N$ is the configurations space of the robot. Assuming that the joints of the robot are actuated, the subspace $\mathcal{Q}_\phi$ contains the actuated dynamics of the system, while the subspace $\mathcal{Q}_N$ contains the unactuated dynamics of the system. Any trajectory in the subspace $\mathcal{Q}_N$ represents a *rigid motion* of the robot, i.e. one where the joint angles are kept constant.
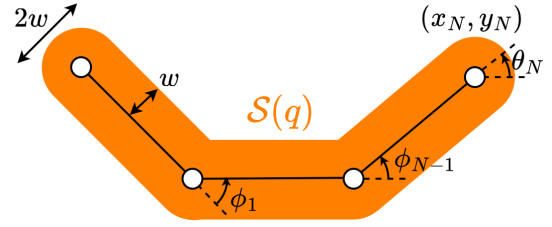

Fig. 2. A kinematic and geometric model of an articulated planar snake robot with $N = 3$ links.

The body of the robot occupies an open, bounded and simply connected region $\mathcal{S}(\boldsymbol{q}) : \mathcal{Q} \mapsto \mathcal{W}$. We define $\mathcal{S}$ as the set of all points whose distance to the spine is less than w. The distance $2w$ is consequently also the width of the robot's body. As the configuration $\boldsymbol{q}$ provides a full parametrization of the robot, any connected trajectory $\boldsymbol{q}(t) : \mathcal{T} \mapsto \mathcal{Q}$ corresponds to a connected physical motion of the snake robot in the workspace $\mathcal{W}$. With the additional constraint that $\boldsymbol{q}(t)$ is twice differentiable with respect to time, the trajectory represents a physically realizable motion with finite generalized forces in the absence of obstacles.

The workspace $\mathcal{W}$ may be cluttered by a series of obstacles that occupy a closed, bounded and possibly disconnected set $\mathcal{O} \subset \mathcal{W}$. Using the above definitions, we define:

Definition 1: A configuration $\boldsymbol{q} \in \mathcal{Q}$ is *penetrating* if the body of the robot and the obstacles overlap, i.e. that

$$\mathcal{O} \cap \mathcal{S}(\boldsymbol{q}) \neq \emptyset.$$

Intuitively, any penetrating configuration is not physically realizable, and the presence of obstacles thus constrains the configuration of the robot. We define the *feasible region* as follows:

Definition 2: The *feasible region* $\mathcal{F} \subset \mathcal{Q}$ is the region of all non-penetrating configurations such that

$$\mathcal{F} = \{\boldsymbol{q} \in \mathcal{Q} \quad | \quad \mathcal{O} \cap \mathcal{S}(\boldsymbol{q}) = \emptyset\}.$$

The complement to the feasible region, $\mathcal{F}' = \mathcal{Q} \setminus \mathcal{F}$, consequently denotes the region of physically infeasible configurations. For each set of joint angles $\boldsymbol{\phi}$ there exists a (possibly empty) set of feasible poses $\mathcal{F}_N(\boldsymbol{\phi}) \subset \mathcal{Q}_N$ that we define as

$$\mathcal{F}_N(\boldsymbol{\phi}) = \{\boldsymbol{q}_N \in \mathcal{Q}_N \quad | \quad (\boldsymbol{\phi}, \boldsymbol{q}_N) \in \mathcal{F}\}.$$

Similarly, we can define a set of physically infeasible poses $\mathcal{F}'_N(\boldsymbol{\phi}) = \mathcal{Q}_N \setminus \mathcal{F}_N(\boldsymbol{\phi})$ for a given set of joint angles.

IV. FORM CLOSURE AND FORM BOUNDEDNESS FOR SNAKE ROBOTS

The overarching goal of form closure analysis in the present context is to determine if, starting from a given configuration, any continuous rigid motion of the robot is possible without causing a penetrating configuration. If this is not the case, the snake robot is under *form closure* and its unactuated dynamics are completely constrained by its contact with the obstacles.
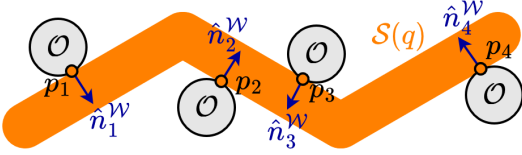
Fig. 3. A simple articulated snake robot $\mathcal{S}(q)$ with $N = 3$ links in a workspace $\mathcal{W} = \mathbb{R}^2$ that is under form closure from the obstacles in its environment.

Fig. 4. A tethered robot manipulator in $\mathcal{W}$ where $\mathcal{W} = \mathbb{R}^2$ accompanied by an untethered block (orange). The system has an identical configuration space representation to a snake robot.

A simple example of a robot under form closure is shown in Fig. 3.

All possible rigid motions of the robot are encoded in the model by the subspace $\mathcal{Q}_N$. If, for a given pose $\boldsymbol{q}_N$, all neighboring points of $\boldsymbol{q}_N$ are infeasible, then there exists no rigid motion that would not cause a penetrating configuration. We can formalize this as follows:

Definition 3: A snake robot is *under form closure* in the configuration $\boldsymbol{q} = (\boldsymbol{\phi}, \boldsymbol{q}_N)$ if, and only if, $\boldsymbol{q}_N$ is an isolated point of $\mathcal{F}_N(\boldsymbol{\phi})$.

The region of all configurations that are under form closure can then be defined accordingly:

Definition 4: *The form closed region* $\mathcal{F}^{FC} \subset \mathcal{F}$ *is the region of all configurations* $\boldsymbol{q}$ *where the snake robot is under form closure.*

The form closed region is a subset of the boundary of the free region as one intuitively needs contact with the environment to be able to achieve form closure. The above definitions allow us to investigate the properties of the form closed region. We propose that:

Definition 5: A continuous trajectory $\boldsymbol{q}(t)$ is *form closed* if it is embedded in the form closed region, i.e. that $\boldsymbol{q}(t) : \mathcal{T} \mapsto \mathcal{F}^{FC}$.

Theorem 1: Consider a form closed trajectory $\boldsymbol{q}^d(t)$ where $\boldsymbol{q}^d(t) = \left(\boldsymbol{\phi}^d(t), \boldsymbol{q}_N^d(t)\right)$. If a snake robot with a configuration $\boldsymbol{q}(t) = (\boldsymbol{\phi}(t), \boldsymbol{q}_N(t))$ is placed such that $\boldsymbol{q}(0) = \boldsymbol{q}^d(0)$ and actuated by $\boldsymbol{\phi}(t) = \boldsymbol{\phi}^d(t)$, then it follows that $\boldsymbol{q}_N(t) = \boldsymbol{q}_N^d(t)$ for all $t \in \mathcal{T}$.

From a geometric perspective, the above states that if a snake robot is placed in an initial form closed configuration $\boldsymbol{q}^d(0)$ and actuated along a desired form closed trajectory by the joint angle sequence $\boldsymbol{\phi}^d(t)$, its pose is completely determined by the joint angle sequence for the entirety of the trajectory. The proof of the above theorem follows from Definition 3: any departure of the head pose $\boldsymbol{q}_N(t)$ from the desired head pose $\boldsymbol{q}_N^d(t)$ would have to enter the infeasible region $\mathcal{F}_N'(\phi)$ as $\boldsymbol{q}_N^d(t)$ is an isolated point in $\mathcal{F}_N(\phi)$. It follows from Theorem 1 that:

Corollary 1.1: When limited in motion to the form closed region $\boldsymbol{q} \in \mathcal{F}^{FC}$, the representation of system's configuration space is constrained from $\mathbb{R}^{N-1} \times \mathrm{SE}(2)$ to $\mathbb{R}^{N-1}$.
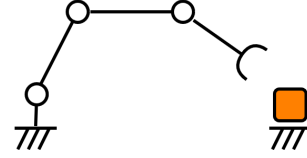
Corollary 1.2: When limited in motion to the form closed region $\boldsymbol{q} \in \mathcal{F}^{FC}$, the system is fully actuated.

The above statements might best be understood by studying a similar system parameterized by the same configuration space. Consider a tethered planar robot manipulator of $N - 1$ links with a gripper on the end accompanied by an untethered block, as shown in Fig. 4. Assume that the gripper is capable of producing a form closed grasp on the block, and that we disregard the kinematics of the gripper itself. The configuration space of the system is given by the $N - 1$ joints of the manipulator and the free motion of the block. Thus the system's configuration space can be represented by the space $\mathbb{R}^{N-1} \times \mathrm{SE}(2)$, identical to that of the snake robot.

If the manipulator grips the block, the system is constrained, and the motion of the block is completely determined by the motion of the manipulator. In this case, the configuration space of the constrained system is $\mathbb{R}^{N-1}$. This notion is transferable to a snake robot where the unactuated motion is that of the untethered snake robot and form closure is achieved by contact with fixed obstacles instead of using a gripper.

An important feature of the form closed region is the possibility for locomotion by slithering. Form closure is strictly a property of the robots' contact points with the obstacles and the geometry of the bodies in the vicinity of these points. The snake robot can slide along the obstacles while still remaining in form closure, although this might seem counter-intuitive given that the goal of form closure is to immobilize the snake robot. This is made possible by performing motions that do not change the geometry around the contact points. This feature is examined further in Section VI.

While the kinematic constraints on the snake robot in general are non-holonomic due to discontinuous contact with obstacles, we can make some assumptions on the constraints when limiting our motion to the form closed region. In the general case, the dynamics of the pose $\boldsymbol{q}_N$ is highly non-linear. Its dynamics are unactuated, and is determined by the internal dynamics of the robot, in conjunction with the external forces acting on the robot from the obstacles [9]. Consequentially, it is difficult to determine whether a given actuation may cause the robot to lose any of its current contact points with its environment. We propose that

Theorem 2: When under form closure, no motion in the unactuated subspace $\mathcal{Q}_N$ can cause a snake robot to depart from a contact point.

Theorem 2 implies that it is impossible to "accidentally" lose contact with an obstacle due to the unactuated dynamics
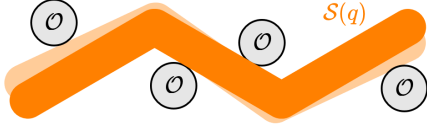
Fig. 5. An articulated snake robot $\mathcal{S}(q)$ with $N = 3$ links in a workspace $\mathcal{W} = \mathbb{R}^2$ that is form bounded by the obstacles in its environment. The lightly shaded geometry shows an alternative pose of the robot reachable through a rigid motion.
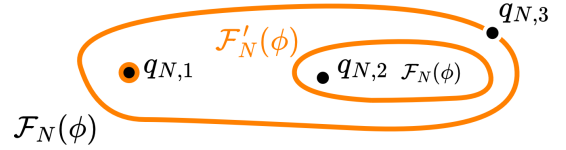

Fig. 6. A visual representation of three different head poses in c-space. The pose $\boldsymbol{q}_{N,1}$ is under form closure as it is an isolated point of $\mathcal{F}_N(\boldsymbol{\phi})$. The pose $\boldsymbol{q}_{N,2}$ is form bounded as its connected component is bounded. Finally, $\boldsymbol{q}_{N,3}$ has neither form closure nor form boundedness.

of the robot. Whether or not the snake robot departs from an obstacle is given entirely by its actuated dynamics. The proof of the theorem follows directly from Definition 3, as any motion in $\mathcal{Q}_N$ when under form closure would cause the robot to enter the physically infeasible region $\mathcal{F}'_N(\boldsymbol{\phi})$. Form closure is a strict condition requiring the head pose $\boldsymbol{q}_N$ to be completely enclosed by $\mathcal{F}'_N(\boldsymbol{\phi})$, which in theory would require perfect knowledge of the geometry of the snake robot's environment and of the robot itself. In a real-life scenario, the joint angles might deviate slightly from their desired values, the body of the snake might deform under load, the estimated position of the obstacles might be inaccurate or the obstacles might shift under interaction. As such, form closure in its strictest mathematical sense is nearly impossible to achieve, making a control strategy based on strict form closure fragile. To address this problem we introduce the relaxed condition of *form boundedness* and define:

Definition 6: A snake robot is *form bounded* in the configuration $\boldsymbol{q} = (\boldsymbol{\phi}, \boldsymbol{q}_N)$ if the connected component of $\boldsymbol{q}_N$ in $\mathcal{F}_N(\boldsymbol{\phi})$ is bounded.

One such configuration is shown in Fig. 5. A robot that is form bounded, as opposed to form closed, is allowed some "wiggle room" around its current pose, but cannot leave a certain neighborhood of its current configuration without causing a penetration. Form closure is indeed a special case of form boundedness where the connected component contains only $\boldsymbol{q}_N$. This allows us to define a region of form bounded configurations and trajectories:

Definition 7: The *form bounded region* $\mathcal{F}^{FB} \subset \mathcal{F}$ is the set of all configurations $\boldsymbol{q}$ that are form bounded.

Definition 8: A trajectory $\boldsymbol{q}(t)$ is *form bounded* if it is embedded in the form bounded region such that $\boldsymbol{q}(t) : \mathcal{T} \mapsto \mathcal{F}^{FB}$

The above definition allows us to restate Theorem 1 in terms of form boundedness as:

Theorem 3: Consider a form bounded trajectory $\boldsymbol{q}^d(t)$, where $\boldsymbol{q}^d(t) = (\boldsymbol{\phi}^d(t), \boldsymbol{q}_N^d(t))$. If a snake robot with a configuration $\boldsymbol{q}(t) = (\boldsymbol{\phi}(t), \boldsymbol{q}_N(t))$ is placed such that $\boldsymbol{q}(0) = \boldsymbol{q}^d(0)$ and actuated by $\boldsymbol{\phi}(t) = \boldsymbol{\phi}^d(t)$, then it follows that $\boldsymbol{q}_N(t)$ remains in the connected component of $\boldsymbol{q}_N^d(t)$ for all t in $\mathcal{T}$.

This implies that, when form bounded, the robot will remain within some bounded neighborhood of its desired trajectory, although it may not track the desired path perfectly. The proof is conceptually similar to that of Theorem 1, as any $\boldsymbol{q}_N(t)$

leaving the connected component of $\boldsymbol{q}_N^d(t)$ would require $\boldsymbol{q}_N$ to enter $\mathcal{F}'_N(\boldsymbol{\phi})$, as the connected component is bounded by $\mathcal{F}'_N(\boldsymbol{\phi})$.

A visual representation of the different forms of boundedness is shown in Fig. 6. Unlike form closure, form boundedness does not guarantee that the constrained system is fully actuated.

V. COMPUTATION OF FORM CLOSURE

The form closure problem is complex, as the obstacles may have complex geometries. Because of this, there is no general method for determining whether a configuration is form closed. This again implies that there exists no general method for analytically determining the form closed region. Methods exist that allows for form closure computation for a large subset of scenarios using approximations of the involved geometries, which will be studied further in the following subsection.

These methods rely on an approximation of the geometry of the robot and the obstacles in the vicinity of their contact points. The methods can be structured into a hierarchy based on the order of the approximation that is used, and are thus called n^{th} *order form closure*. As the order of the approximation decreases, the conditions for achieving n^{th} order form closure become increasingly strict, but allows for stronger assumptions on the properties of the configuration.

The most widely adapted approximations is that of 1st order form closure [24]. In this case we study whether an instantaneous rigid motion $\dot{\boldsymbol{q}}_N \in \dot{\mathcal{Q}}_N$ of the robot will cause a penetration of at least one obstacle. These motions are commonly referred to as *twists* and the space $\dot{\mathcal{Q}}_N$ as the *twist space* [25].

We denote the contact points between the robot and the obstacles as $\boldsymbol{p}_1 \cdots \boldsymbol{p}_k \in \mathcal{S}(\boldsymbol{q})$ as shown in Fig. 3. Each of the contact points is assigned a *contact normal vector* $\hat{\boldsymbol{n}}_1^{\mathcal{W}} \cdots \hat{\boldsymbol{n}}_k^{\mathcal{W}} \in \mathcal{W}$ that are unit vectors that are normal to the boundary of the robot in each respective contact point and oriented away from the obstacle.

The velocity of each contact point $\dot{\boldsymbol{p}}_i$ when subject to a twist parameterized by $\dot{\boldsymbol{q}}_N = (\dot{\boldsymbol{x}}_N, \dot{\boldsymbol{y}}_N, \dot{\boldsymbol{\theta}}_N)$ is known to be

$$\dot{\boldsymbol{p}}_i = [\dot{\boldsymbol{\theta}}]_\times \hat{\boldsymbol{p}}_i + [\dot{\boldsymbol{x}}_N, \dot{\boldsymbol{y}}_N]^T \tag{3}$$

where $[\cdot]_\times$ denotes the skew symmetric matrix of a given vector. The nature of the interaction at a given contact point is implied by the product $\dot{\boldsymbol{p}}_i \cdot \hat{\boldsymbol{n}}_i^{\mathcal{W}}$, where the operator $(\cdot)$
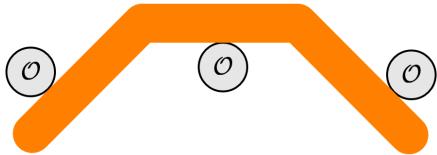
Fig. 7. An articulated snake robot whose unactuated dynamics are immobilized by the obstacles, but which is not under 1st order form closure

denotes the dot product. If the product is positive, the robot is moving away from the obstacle in the given contact point. If the product is zero, the robot slides or rolls along the obstacle. If the product were negative, the robot would penetrate the obstacle at the given contact point. Thus, each contact point imparts a constraint

$$\dot{\boldsymbol{p}}_i \cdot \hat{\boldsymbol{n}}_i^{\mathcal{W}} \geq 0. \tag{4}$$

By inserting (3) into (4), the constraint can be written in therms of the twist $\dot{\boldsymbol{q}}_N$ as

$$\dot{\boldsymbol{q}}_N \cdot \hat{\boldsymbol{n}}_i \geq 0 \quad | \quad \hat{\boldsymbol{n}}_i = \left[\boldsymbol{p}_i \left[1\right]_\times \hat{\boldsymbol{n}}_i^{\mathcal{W}}, \, \hat{\boldsymbol{n}}_i^{\mathcal{W}} \right] \in \dot{\mathcal{Q}}_N. \tag{5}$$

This equation defines a half-space in the twist space with $\hat{\boldsymbol{n}}_i$ as its defining normal vector; we denote this half-space $\mathcal{N}_i \subset \dot{\mathcal{Q}}_N$ where

$$\mathcal{N}_i = \{ \dot{\boldsymbol{q}}_N \in \dot{\mathcal{Q}}_N \quad | \quad \dot{\boldsymbol{q}}_N \cdot \hat{\boldsymbol{n}}_i \geq 0 \}. \tag{6}$$

Any applied twist outside $\mathcal{N}_i$ would constitute a penetration at the ith contact point. The intersection of the half-spaces associated with all contact points yields a region of twists that do not violate any of the constraints. The resulting space

$$\mathcal{V} = \bigcap_{i=1}^{k} \mathcal{N}_i \tag{7}$$

forms a *polyhedral cone* [26]. If the cone contains only its origin, i.e. that $\mathcal{V} = \{\boldsymbol{0}\}$, then no non-zero twists exist that would not cause a penetration. In this case the robot is under 1st order form closure in the configuration $\boldsymbol{q}$. 1st order form closure has the advantage that it guarantees the finiteness of the reaction forces between the robot and the obstacles when subject to a finite external force, but it requires a minimum of four unique contact points in the planar case [24]. A numerical method for determining 1st order form closure is covered in [5], and thus will not be covered further in this paper.

First order form closure is a sufficient condition for form closure in its general sense, however there exist configurations that are form closed that are not 1st order form closed. This implies that 1st order form closure is a conservative metric, as it identifies only a subset of form closed configurations. One such example is shown in Fig. 7. In these cases, a higher order analysis is necessary to determine the closure properties of the robot.

Higher order form closure is covered to a great extent in [27]. Under these analyses, additional derivatives (e.g. $\ddot{\boldsymbol{q}}_N$, $\dddot{\boldsymbol{q}}_N$) are taken into account, and the curvature of the obstacles and the robot around the contact points are considered. Higher order form closure is achievable with a minimum two

contact points in the planar case, and with a minimum of three contact points if the contact points are only on the flat sides of the robot's links [28]. Higher order analysis does not give any guarantees as to the finiteness of the reaction forces, and are significantly more difficult to calculate [27]. Because of the guarantee of finite reaction forces and its computational simplicity, we consider 1st order form closure as the most relevant in the study of snake locomotion.

VI. SIMULATION CASE STUDY

The following case study aims at demonstrating the predictable behavior of a snake robot when locomoting in a form closed region, and how its dynamics are affected when leaving the region. The study takes place in a simulated cluttered 2D environment.

We are specifically studying a form of OAL known as *lateral undulation* [2], [29], which is illustrated in Fig. 8. During lateral undulation, the robot slithers along obstacles in a manner such that every point on its body trails the position of its head, with minimal lateral slippage. It achieves this by propagating the geometry of its body from its head towards its tail. We refer to the path traced by the snake robot's body during locomotion as the *undulation path*.

Lateral undulation is the preferred mode of propulsion for biological snakes [30]. As they undulate through cluttered terrain, the snakes tend to chose their contact points with their environment in a way that is beneficial for their locomotion. Intuitively, there exist configurations where a lateral undulation gait would push the snake off its undulation path or cause the snake to lose propulsion entirely. Biological snakes actively choose paths through their environment that prevent these kinds of configurations [31]. To produce meaningful locomotion with lateral undulation in snake robots, a geometric condition that identifies these kinds of undulation paths and configurations is needed. Form closure can be used for this purpose.

The demonstration builds on a physics based simulation run on the MuJoCo physics engine [32]. The intended undulation path and the position of the obstacles are shown in Fig. 9, and are designed so that the snake robot will remain in the form closed region for an initial portion of the path and exit the form closed region as $t > 31.0s$. The robots' trajectory is designed to provide 1st order form closure. The physical
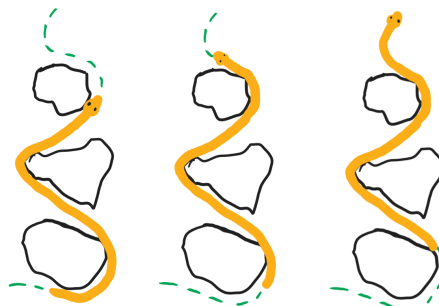

Fig. 8. A snake (orange) moving along a path (dashed green) in an environment cluttered with obstacles (black) by lateral undulation.

parameters of the simulated robot are given in Table I, and were chosen to resemble the Boa snake robot [33].

TABLE I
PHYSICAL PARAMETERS OF THE SIMULATED SNAKE ROBOT

Parameter	Value	Unit
Number of links (N)	15	(unitless)
Link length	0.2	m
Link width ($2w$)	0.16	m
Friction coefficient	0.1	(unitless)
Link mass	0.4	kg
Maximum actuator torque	3	Nm

As the undulation path is continuous it is, in general, not possible to overlay an articulated snake robot perfectly on the path. We utilized the method described in [34], where the head of the robot is placed on the path in a desired position and each joint is consecutively placed on the path behind the head as shown in Fig. 9. By doing this form of approximation, it is a matter of simple geometry to calculate the desired joint angles for any placement of the robot on the path. The path itself is chosen manually while employing the following considerations:

1) The undulation path is straight within a link length's radius of each obstacle. This is to ensure that the joints of the robot are straight as they slide past the obstacle to prevent discontinuities and collisions.
2) The path is created from straight line segments and arcs of constant radius. This is a pattern commonly seen in biological snakes [31] as they attempt to form the shortest possible path between two contact points, but are restricted by a minimum curvature in their body.

Under form closure, the speed at which the shape of the snake robot is propagated backwards along its body is approximately equal to the propulsive speed of the robot's head along the undulation path. In biological snakes this speed typically remains constant during locomotion [35] and as such is set to a constant speed of 0.1 m/s for the following demonstration.

The simulated robot's joint angles $\phi(t)$ are driven to the desired joint angles $\phi^d(t)$ by a monovariable PD control loop in each joint. While this is a naive approach to the low-level control of the robot, it serves to show the efficacy of form closure as a condition for undulation-based locomotion, even when using simple low-level controllers. This controller configuration also guarantees dissipativity and thus rudimentary
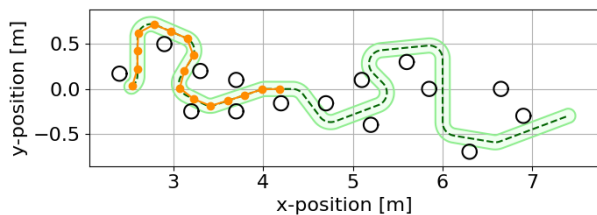
stability properties of the overall system. Renderings of the simulation are shown in Fig. 10. The trajectory of the robot's head compared to its desired position on the undulation path is shown in Fig. 11, and its deviation from the desired head position is shown in Fig. 12. The actuator torque applied throughout the simulation is shown in Fig. 13.

As seen in Fig. 10–12, the robot follows the undulation path when applying a lateral undulation gait as long as it remains in the form closed region. The tracking error between the head position and its desired position remains largely between 0.05 m and 0.1 m. While the across-path error remains relatively small, the error mainly arises from the head lagging slightly behind its desired position along the path. This is likely due to friction and the inability of the PD control loop to perfectly track the desired joint angles $\phi^d(t)$.

As the robot loses form closure at $t = 31.0$ s, it rapidly deviates from the undulation path, as shown in Fig. 11. In Fig. 10, the robot shows significant lateral slippage after losing form closure.

Fig. 13 shows that during locomotion, the actuation of the joints remains under the saturation limit of 3.0 Nm. The average absolute actuation torque can be taken as a proxy for energy expenditure. After an initial transient this graph exhibits a general trend of tapering off after form closure is lost, reflecting that the robot is mostly wiggling in one place while spending little or no energy on gross propulsion. Some oscillations are apparent in the actuation, which can partially be attributed to the presence of friction in the simulation.
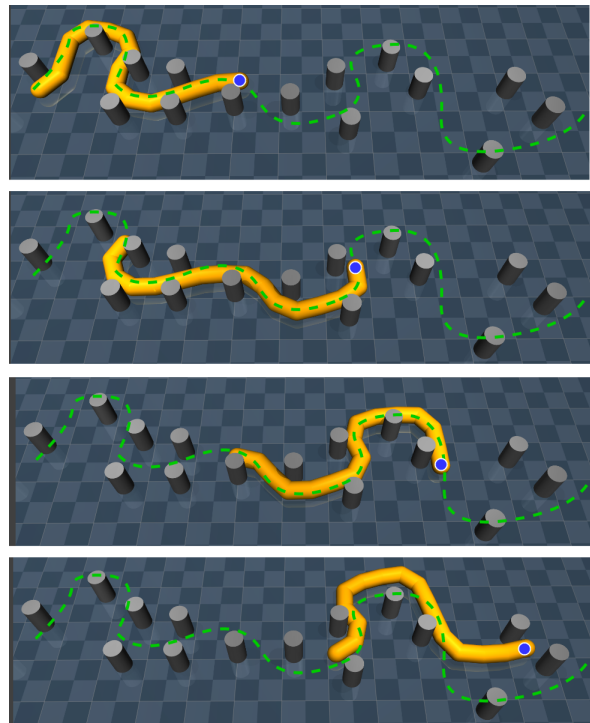

Fig. 9. The undulation path followed by the snake robot in the demonstration. The path itself is marked as an dashed green line with a shaded area showing the area ideally traced by the snake robots' body as it moves along the path. The cylindrical obstacles are marked by black circles. The initial configuration of the snake robots' spine is shown by orange connected circles.

Fig. 10. Still-frames from the simulation showing the locomotion of the snake robot through the cluttered planar environment at times $t =$ 0s, 15s, 30s, 40s. The dashed green line shows the undulation path of the snake robot and the blue circle shows the location of the robots' head.
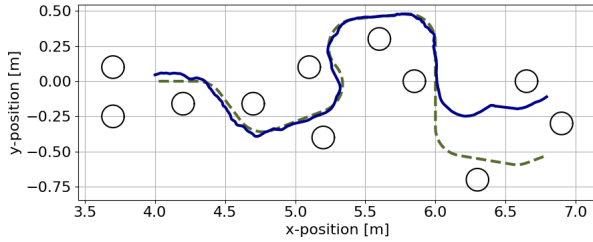
Fig. 11. The blue line shows the position of the snake robots' head, while the dashed line shows the undulation path. The robot loses form closure as the head passes the point $\boldsymbol{p}_N = (6, 0)$.
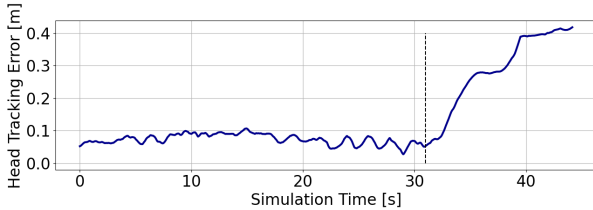

Fig. 12. The blue line shows the euclidean distance from the head position $\boldsymbol{p}_N$ to its desired position along the undulation path. The dashed line at $t = 31.0$ indicates the time when the snake robot loses form closure.
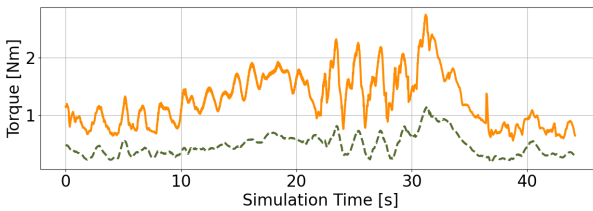

Fig. 13. The dashed line shows the average absolute actuation torque of the joints over time. The orange line shows the actuation of the joint with the greatest actuation torque at any given time.

VII. DISCUSSION AND FUTURE WORKS

While this paper focused on planar snake robots within $\mathcal{W} = \mathbb{R}^2$, all theorems in this paper can be generalized to snake robots operating in $\mathcal{W} = \mathbb{R}^3$ where the space of head poses $\mathcal{Q}_N$ is expanded to so that it is represented by the space $\mathrm{SE}(3)$. In this case it is required to have a minimum of seven contact points between a snake robot and its environment to achieve 1st order form closure. While the complexity of calculating form closure increases in a 3-dimensional workspace, the structure of the form closure problem remains similar. Thus, the findings in this paper are relevant even when studying snake robots in three dimensions, and should lend itself to further generalization to non-snake-like robot OAL.

As form closure is a strictly geometric condition, it does not consider friction. The effect of this is twofold: Form closure guarantees that the unactuated dynamics of the snake robot are constrained, even when friction is near nonexistent. On the other hand, there intuitively exist form closed configurations where an attempted motion would cause the propulsive forces to be canceled out by equal frictional reaction forces from the obstacles. In this case the robot would be jammed in its current configuration. Consequently, a form closed configuration does not guarantee that locomotion is possible in a scenario with friction. The resolution of jammed configurations is treated in some detail in [7], but further research is necessary to identify criteria for jam avoidance.

Biological snakes are often observed to produce undulatory locomotion in cluttered environments using three or less contact points, and in some cases using only a single contact point [29]. This alludes that form closure is an overly strict condition, and that there exist less strict conditions that still allow for undulatory locomotion. Of particular interest are the notions of *partial form closure* and *force closure* [5], [36].

In this paper we treated form boundedness from a purely mathematical perspective. As this is a novel concept, further research may be done in developing analytical or numerical methods for identifying form bounded configurations. We also recognize a limitation of form boundedness: The loss of form closure in a given configuration does not guarantee that it will become form bounded before losing its constrainedness entirely.

Although form closure is a well-researched topic, to the best of the authors' knowledge this work is novel in utilizing form closure as a condition for locomotion. The development of path planning algorithms and of control strategies that build on the concepts of form closure go beyond the scope of this manuscript, and constitute an interesting topic for future research. Possible directions for this research include energy optimal path planning in the presence of a hierarchy of constraints related to form closure, form boundedness and other, increasingly relaxed criteria. One possible goal of such an endeavor is to ensure graceful degradation of the system's propulsive abilities in the presence of an uncertain or unpredictable environment.

ACKNOWLEDGMENT

REFERENCES

[1] J. Liu, Y. Tong, and J. Liu, "Review of snake robots in constrained environments," *Robotics and Autonomous Systems*, vol. 141, p. 103785, 2021. [Online]. Available: https://www.sciencedirect.com/science/article/pii/S0921889021000701

[2] J. Gray, "The mechanism of locomotion in snakes," *Journal of experimental biology*, vol. 23, no. 2, pp. 101–120, 1946.

[3] A. A. Transeth, R. I. Leine, C. Glocker, K. Y. Pettersen, and P. LiljebÄck, "Snake robot obstacle-aided locomotion: Modeling, simulations, and experiments," *IEEE Transactions on Robotics*, vol. 24, no. 1, pp. 88–104, 2008.

[4] E. Rimon and J. Burdick, "On force and form closure for multiple finger grasps," in *Proceedings of IEEE International Conference on Robotics and Automation*, vol. 2, 1996, pp. 1795–1800 vol.2.

[5] A. Bicchi, "On the closure properties of robotic grasping," *The International Journal of Robotics Research*, vol. 14, no. 4, pp. 319–334, 1995.

[6] A. Bicchi and V. Kumar, "Robotic grasping and contact: A review," in *Proceedings 2000 ICRA. Millennium conference. IEEE international conference on robotics and automation. Symposia proceedings (Cat. No. 00CH37065)*, vol. 1. IEEE, 2000, pp. 348–353.

[7] P. Liljeback, K. Pettersen, and O. Stavdahl, "Modelling and control of obstacle-aided snake robot locomotion based on jam resolution," in *IEEE International Conference on Robotics and Automation*, 06 2009, pp. 3807 – 3814.

[8] P. Liljeback, K. Y. Pettersen, O. Stavdahl, and J. T. Gravdahl, "Hybrid modelling and control of obstacle-aided snake robot locomotion," *IEEE Transactions on Robotics*, vol. 26, no. 5, pp. 781–799, 2010.

[9] P. Liljebäck, K. Y. Pettersen, Ø. Stavdahl, and J. T. Gravdahl, *Snake robots: modelling, mechatronics, and control.* Springer Science & Business Media, 2012.

[10] I. Gravdahl, Øyvind Stavdahl, A. Koushan, J. Løwer, and K. Y. Pettersen, "Modeling for hybrid obstacle-aided locomotion (hoal) of snake robots," *IFAC-PapersOnLine*, vol. 55, no. 20, pp. 247–252, 2022, 10th Vienna International Conference on Mathematical Modelling MATHMOD 2022. [Online]. Available: https://www.sciencedirect.com/science/article/pii/S2405896322012940

[11] T. Takanashi, M. Nakajima, T. Takemori, and M. Tanaka, "Obstacle-aided locomotion of a snake robot using piecewise helixes," *IEEE Robotics and Automation Letters*, vol. 7, no. 4, pp. 10542–10549, 2022.

[12] B. Chong, T. Wang, D. Irvine, V. Kojouharov, B. Lin, H. Choset, D. I. Goldman, and G. Blekherman, "Gait design for limbless obstacle aided locomotion using geometric mechanics," 2023.

[13] T. Takemori, M. Tanaka, and F. Matsuno, "Hoop-passing motion for a snake robot to realize motion transition across different environments," *IEEE Transactions on Robotics*, vol. 37, no. 5, pp. 1696–1711, 2021.

[14] K. G. Hanssen, A. A. Transeth, F. Sanfilippo, P. Liljebäck, and O. Stavdahl, "Path planning for perception-driven obstacle-aided snake robot locomotion," in *2020 IEEE 16th International Workshop on Advanced Motion Control (AMC)*, 2020, pp. 98–104.

[15] B. A. Elsayed, T. Takemori, M. Tanaka, and F. Matsuno, "Mobile manipulation using a snake robot in a helical gait," *IEEE/ASME Transactions on Mechatronics*, vol. 27, no. 5, pp. 2600–2611, 2022.

[16] D. Li, Z. Pan, H. Deng, and L. Hu, "Adaptive path following controller of a multijoint snake robot based on the improved serpenoid curve," *IEEE Transactions on Industrial Electronics*, vol. 69, no. 4, pp. 3831–3842, 2022.

[17] T. Takemori, M. Tanaka, and F. Matsuno, "Adaptive helical rolling of a snake robot to a straight pipe with irregular cross-sectional shape," *IEEE Transactions on Robotics*, vol. 39, no. 1, pp. 437–451, 2023.

[18] I. Virgala, M. Kelemen, E. Prada, M. Sukop, T. Kot, Z. Bobovský, M. Varga, and P. Ferenčík, "A snake robot for locomotion in a pipe using trapezium-like travelling wave," *Mechanism and Machine Theory*, vol. 158, p. 104221, 2021. [Online]. Available: https://www.sciencedirect.com/science/article/pii/S0094114X20304389

[19] G. Qin, H. Wu, Y. Cheng, H. Pan, W. Zhao, S. Shi, Y. Song, and A. Ji, "Adaptive trajectory control of an under-actuated snake robot," *Applied Mathematical Modelling*, vol. 106, pp. 756–769, 2022. [Online]. Available: https://www.sciencedirect.com/science/article/pii/S0307904X22000646

[20] F. Reyes and S. Ma, "Snake robots in contact with the environment: Influence of the configuration on the applied wrench," in *2016 IEEE/RSJ International Conference on Intelligent Robots and Systems (IROS)*. IEEE, 2016, pp. 3854–3859.

[21] ——, "Studying slippage on pushing applications with snake robots," *Robotics and Biomimetics*, vol. 4, no. 1, pp. 1–12, 2017.

[22] ——, "On planar grasping with snake robots: Form-closure with enveloping grasps," in *2014 IEEE International Conference on Robotics and Biomimetics (ROBIO 2014)*. IEEE, 2014, pp. 556–561.

[23] G. Grzancic, C. Löbbe, N. B. Khalifa, and A. E. Tekkaya, "Analytical prediction of wall thickness reduction and forming forces during the radial indentation process in incremental profile forming," *Journal of Materials Processing Technology*, vol. 267, pp. 68–79, 2019.

[24] E. Rimon and J. W. Burdick, "A configuration space analysis of bodies in contact-i. 1st order mobility," *Mechanism and Machine Theory*, vol. 30, pp. 897–912, 1995.

[25] J. K. Davidson, K. H. Hunt, and G. R. Pennock, "Robots and screw theory: applications of kinematics and statics to robotics," *J. Mech. Des.*, vol. 126, no. 4, pp. 763–764, 2004.

[26] S. Hirai, "Analysis and planning of manipulation using the theory of polyhedral convex cones," Ph.D. dissertation, Kyoto University, 1991.

[27] E. Rimon and J. W. Burdick, "A configuration space analysis of bodies in contact-ii. 2nd order mobility," *Mechanism and Machine Theory*, vol. 30, pp. 913–928, 1995.

[28] J. Czyzowicz, I. Stojmenovic, and J. Urrutia, "Immobilizing a polytope," *Workshop on Algorithms and Data Structures*, 1991.

[29] J. Gray and H. W. Lissmann, "The kinetics of locomotion of the grass-snake," *Journal of Experimental Biology*, vol. 26, no. 4, pp. 354–367, 02 1950. [Online]. Available: https://doi.org/10.1242/jeb.26.4.354

[30] C. Gans, "How snakes move," *Scientific American*, vol. 222, no. 6, pp. 82–99, 1970. [Online]. Available: http://www.jstor.org/stable/24925828

[31] P. E. Schiebel, A. M. Hubbard, and D. I. Goldman, "Comparative study of snake lateral undulation kinematics in model heterogeneous terrain." *Integrative and comparative biology*, 2020.

[32] E. Todorov, T. Erez, and Y. Tassa, "Mujoco: A physics engine for model-based control," in *2012 IEEE/RSJ International Conference on Intelligent Robots and Systems*, 2012, pp. 5026–5033.

[33] J. Løwer, I. Gravdahl, D. Varagnolo, and Ø. Stavdahl, "Proprioceptive contact force and contact point estimation in a stationary snake robot," *IFAC-PapersOnLine*, vol. 55, no. 38, pp. 160–165, 2022.

[34] P. Liljeback, K. Y. Pettersen, O. Stavdahl, and J. T. Gravdahl, "A control framework for snake robot locomotion based on shape control points interconnected by bézier curves," in *2012 IEEE/RSJ International Conference on Intelligent Robots and Systems*, 2012, pp. 3111–3118.

[35] B. C. Jayne, "What Defines Different Modes of Snake Locomotion?" *Integrative and Comparative Biology*, vol. 60, no. 1, pp. 156–170, 04 2020. [Online]. Available: https://doi.org/10.1093/icb/icaa017

[36] B. Siciliano, O. Khatib, and T. Kröger, *Springer handbook of robotics*. Springer, 2008, vol. 200.